



**HAL**  
open science

## Buckling and wrinkling during strip conveying in processing lines

Nicolas Jacques, Akli Elias, Michel Potier-Ferry, Hamid Zahrouni

► **To cite this version:**

Nicolas Jacques, Akli Elias, Michel Potier-Ferry, Hamid Zahrouni. Buckling and wrinkling during strip conveying in processing lines. *Journal of Materials Processing Technology*, 2007, 190 (1-3), pp.33-40. 10.1016/j.jmatprotec.2007.03.117 . hal-04758000

**HAL Id: hal-04758000**

**<https://hal.science/hal-04758000v1>**

Submitted on 29 Oct 2024

**HAL** is a multi-disciplinary open access archive for the deposit and dissemination of scientific research documents, whether they are published or not. The documents may come from teaching and research institutions in France or abroad, or from public or private research centers.

L'archive ouverte pluridisciplinaire **HAL**, est destinée au dépôt et à la diffusion de documents scientifiques de niveau recherche, publiés ou non, émanant des établissements d'enseignement et de recherche français ou étrangers, des laboratoires publics ou privés.



Distributed under a Creative Commons Attribution - NonCommercial 4.0 International License

# Buckling and wrinkling during strip conveying in processing lines

N. Jacques<sup>a,\*</sup>, A. Elias<sup>b</sup>, M. Potier-Ferry<sup>c</sup>, H. Zahrouni<sup>c</sup>

<sup>a</sup>Laboratoire de Mécanique des Structures Navales, ENSIETA, 2 rue François Verny, 29806 Brest, France

<sup>b</sup>ARCELOR Research SA, Voie Romaine, 57280 Maizières-lès-Metz, France

<sup>c</sup>Laboratoire de Physique et Mécanique des Matériaux (LPMM), UMR CNRS 7554, Université Paul Verlaine Metz, Ile du Saulcy, 57045 Metz, France

This paper deals with the occurrence of plastic creases, called wrinkles, in a strip travelling through a continuous processing line. During this process, strips run over numerous rolls under global tension. Finite element analyses are carried out to model the formation of wrinkles when a strip is passing over a roll. When the strip is stretched, transverse compressive stresses appear near the roll and cause the strip buckling. Simulations have shown that friction between sheet and roll induces an increase of the amplitude of the buckles. In some cases, a plastic cumulative mechanism is triggered and leads to the occurrence of a wrinkle. A description of these phenomena is proposed.

*Keywords:* Metal sheet; Continuous processing lines; Post-buckling; Wrinkling; Finite element method

## 1. Introduction

In processing lines, sheets of metal are in a continuous form, called strip or web, and travel through the plant. Strips are guided by upper and lower rolls in an alternate up and down vertical motion (Fig. 1). This kind of process has several advantages in terms of productivity and product quality. For example, continuous annealing furnaces allow to control accurately the thermal treatment of strips and to obtain steels having very good mechanical properties. Main problems encountered in continuous strip processing lines are breaks due to misguiding and formation of wrinkles. This paper is focused on the second one. In the context of metal strip conveying, a wrinkle is a plastic crease generally oriented in the strip direction (Fig. 2b). When this phenomenon initiates, sheets must be thrown out. Furthermore, it may cause a strip break inducing a production shutdown of at least 1 day. The economic impact of wrinkling is therefore significant and has to be reduced.

Initiation of wrinkles follows a buckling phenomenon induced by a tensile load, applied in order to avoid strip wandering. Rolls have a convex crown profile, which generates a non-uniform tension distribution across the strip width and the

occurrence of lateral compressive stresses. Since sheets are thin and large, the magnitude of the applied tensile load is generally greater than the critical buckling load. Thus, buckles are present in the web span, i.e. the unsupported strip part between two rolls. Nevertheless, the longitudinal tensile stresses provide a stabilizing effect and the amplitude of buckles remains moderate. Buckling generates only low magnitude stresses. Thus, the yield stress is rarely reached. Therefore, the wrinkling phenomenon cannot be explained by a plastic buckling. Wrinkles formation is observed only during the strip motion, when the strip passes over a roll (Fig. 2a). Thus, mechanisms leading to a strong increase of the buckles amplitude should operate during the strip displacement. In the following, buckles will designate large waves, generally elastic, which affect the web span, and wrinkles, plastic creases that appear when the strip passes over a roll. Wrinkling occurs when the tension applied to the strip reaches a critical level, called the critical wrinkling load  $T_W$ . The magnitude of  $T_W$  is much larger than the critical buckling load  $T_B$  (Fig. 3). Therefore, in plants, the tension has to be sufficient to prevent strip snaking, but limited under the critical wrinkling load, in order to avoid this phenomenon.

There is some literature dealing with the buckling of structures subjected to tensile loads. Linear buckling analyses have been proposed in order to predict the onset of buckling, i.e. to compute the buckling load  $T_B$ . For thin plates under traction, some studies can be found in Refs. [1–5]. The linear approach

\* Corresponding author. Tel.: +33 2 98 34 89 36; fax: +33 2 98 34 87 30.  
E-mail address: nicolas.jacques@ensieta.fr (N. Jacques).

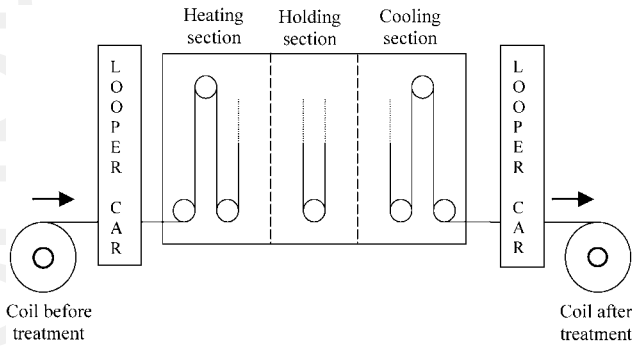


Fig. 1. Schematic view of a continuous annealing line.

has been applied to investigate buckling phenomena occurring in strip processing lines. Sasaki et al. [6] and Matoba [7] have proposed analytical formula for estimating the critical buckling load in continuous annealing lines, where the strip is handled by convex rolls. Luo et al. [8] have performed a numerical study of the thermal buckling in continuous annealing furnaces. Fischer et al. [9] have investigated both buckling due to self-equilibrating stresses generated by the rolling process and occurrence of waviness during the levelling of metal sheets. Using finite element models, Marchand [10] has also studied the occurrence of waviness after sheet metal rolling. Note that only the linear buckling and initial elastic post-buckling were considered in Refs. [9,10].

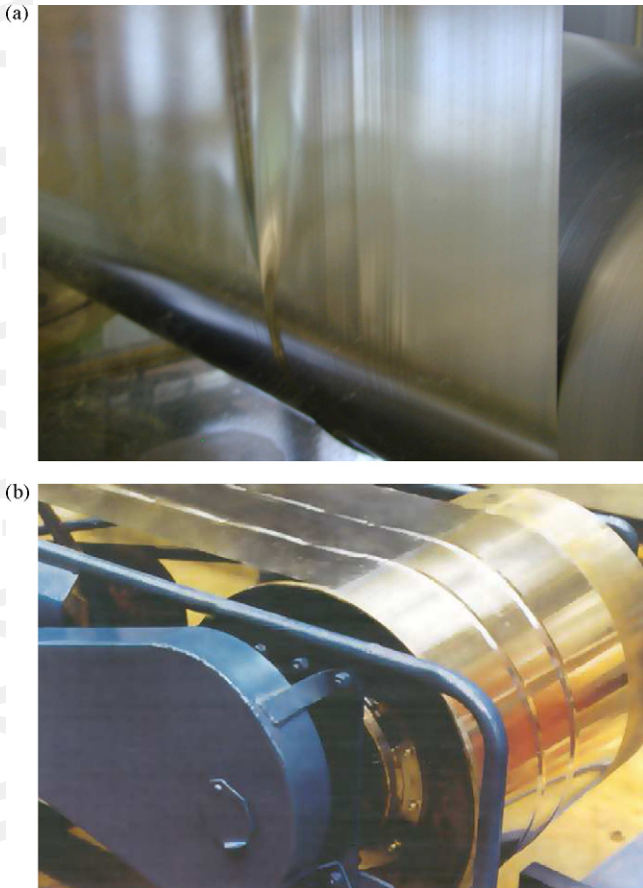


Fig. 2. Experimental observations of wrinkles. Wrinkles occur on a roll (a) and propagate in the downstream web span (b).

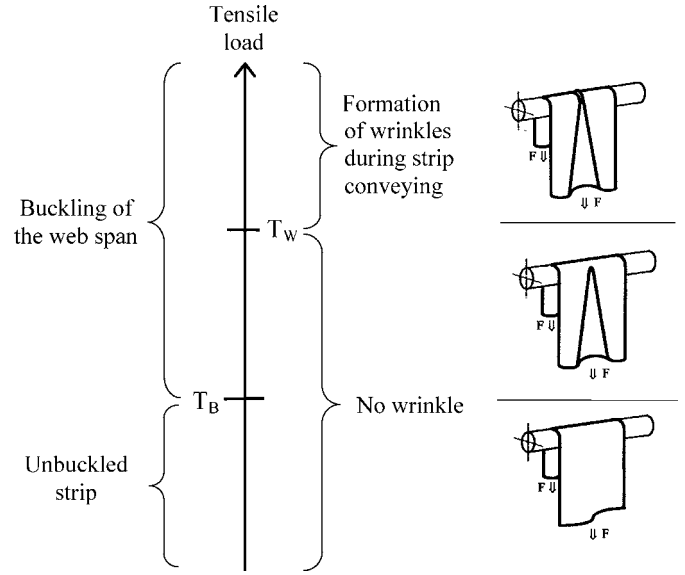


Fig. 3. Buckling and wrinkling during sheet conveying.  $T_B$  is the critical buckling load and  $T_W$  is the critical wrinkling load.

Gueydan [11] has proposed non-linear finite element models to simulate the onset and growth of buckles in continuous annealing lines. Note that these models do not simulate the strip motion. In agreement with earlier works [6,7], Gueydan observed that the main cause of buckling is the convex shape of the rolls. Comparison with experimental results showed that the numerical analyses predict accurately the shape and the amplitude of buckles when unilateral contact between sheet and roll is considered in simulations. However, Gueydan has observed that the stresses induced by the tensile buckling are too low to explain the occurrence of plastic deformation and thus wrinkling. This result reveals the need to carry out realistic simulations of strip conveying.

From the literature, both analytical and numerical models are available for the prediction of buckling during strip processing. The phenomenon of wrinkling is not as well established since, to the authors' knowledge, the effect of the strip displacement has not been previously investigated. In this paper, finite element analyses are proposed to describe the behaviour of a strip running over a roll under global tension. The mechanism of wrinkling is clearly identified and explained. Effects of friction and plasticity are highlighted.

## 2. Finite element model

Numerical investigations of strip conveying are performed with the commercial software ABAQUS/Standard [12]. Non-linear static stress calculations are carried out on a configuration, where only a single roll and a sheet of metal are considered. In the present approach, the sheet is modelled as a thin shell and the roll as a rigid surface. As mentioned before, rolls have a non-uniform cross-section. The diameter of the ends is reduced to improve web guiding. Different rolls profiles may be adopted [6,7,11]. In the present work, tapered rolls, see Fig. 4, are considered since they are widely used in plants. Besides, in some processes

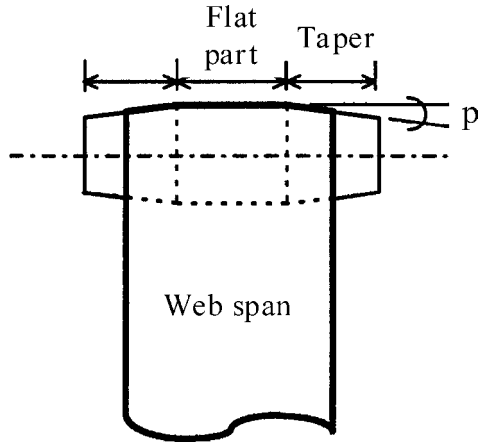


Fig. 4. Geometry of tapered rolls. The parameter  $p$ , named the taper angle, defines the cross-section reduction.

like annealing, the strip is heated in a furnace. Temperatures of the strip and the furnace are different. As a consequence, the roll temperature becomes inhomogeneous leading to a change of the roll geometry. Elias et al. [13] have proposed a thermo-elastic model for the prediction of roll shape variations in annealing furnaces. The effect of the temperature on the roll shape is not investigated in the following.

The strip is meshed using quadratic shell elements with reduced integration, assuming large rotations and displacements but only small strains (ABAQUS S8R5). These elements are dedicated to thin shell problems. Therefore, transverse shear flexibility is neglected. The Simpson integration scheme is used to calculate the shell cross-sectional behaviour. It has been shown that five integration points in the shell thickness are sufficient to obtain accurate results. A mesh convergence study was performed to determine an appropriate mesh density. This study has revealed that the mesh size in the lateral direction is the dominant parameter for the simulation of wrinkling. In order to obtain an accurate solution, at least five elements should be used along the wrinkle width. Fig. 2 shows that this width is small as compared to the strip one. Besides, from simulations, it has been observed that the wrinkle width decreases with the sheet thickness. Therefore, a finer mesh is required for thin sheets. Because of symmetry, only one half of the strip is modelled. A typical mesh is plotted in Fig. 5. In the proposed calculations, the number of degrees of freedom varies from 70,000 to 300,000.

In the present work, the strip material has an isotropic elastic-plastic behaviour with Mises yield surface and associated flow rule.  $E$  denotes the Young modulus and  $\nu$  the Poisson ratio. The hardening behaviour is obtained from uniaxial tensile tests and defined in ABAQUS by providing a set of couples (yield stress, plastic strain). Yield stress at a given state is simply interpolated from this data.

Finite sliding contact is defined between the sheet and the roll. Isotropic Coulomb friction is assumed for the tangential behaviour.

Simulations are performed in two steps. First, a homogeneous longitudinal tensile stress is applied at one end of the sheet, leading to the strip buckling. During the second step, the applied

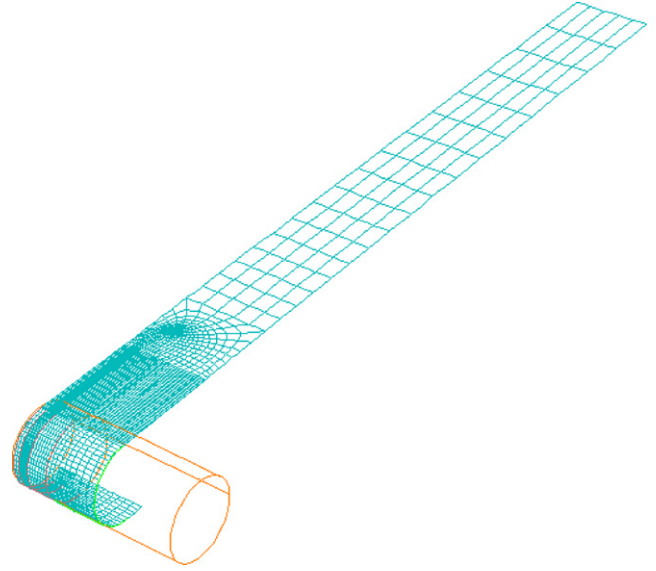


Fig. 5. Typical mesh used in the present work. Owing to symmetry, only one half of the sheet is modelled.

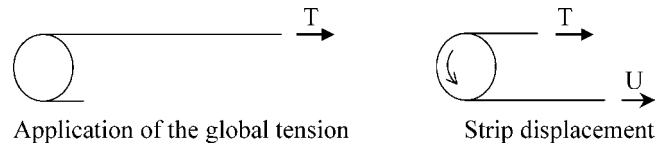


Fig. 6. Presentation of the two-step simulations of strip conveying.

tension remains constant. A uniform displacement is applied to the other end of the strip and a rotation to the roll (Fig. 6). In processing lines, rolls used to convey the strip are free in rotation. Consequently, no longitudinal sliding between sheet and roll is observed. Thus, the displacement of the strip ( $U$ ) and the rotation angle of the roll ( $\alpha$ ), expressed in radians, are linked by the following relationship:

$$U = \alpha R \quad (1)$$

where  $R$  is the roll radius.

In the following, this second step will be named the strip displacement. During this stage, the post-buckling patterns evolve leading for some conditions to the formation of a wrinkle.

### 3. Buckling under global tension

In this part, the buckling observed during the first stage of the simulations is briefly discussed. More details about tension buckling can be found in Refs. [1–5]. Buckling phenomena are due to compressive stresses generated in the present problem by the roll geometry (Fig. 4). Even if the difference of diameters in a tapered roll is usually small (about 1 mm), contact takes place first on the central part of the roll, creating an inhomogeneous stress field with lateral compression. Fig. 7a shows that compressive stresses are localized in a small area near the roll. For an applied tensile membrane force equal to 3.6 N/mm, the magnitude of the compressive membrane forces reaches 2.6 N/mm. In this case, compressive and tensile stresses are of the same order

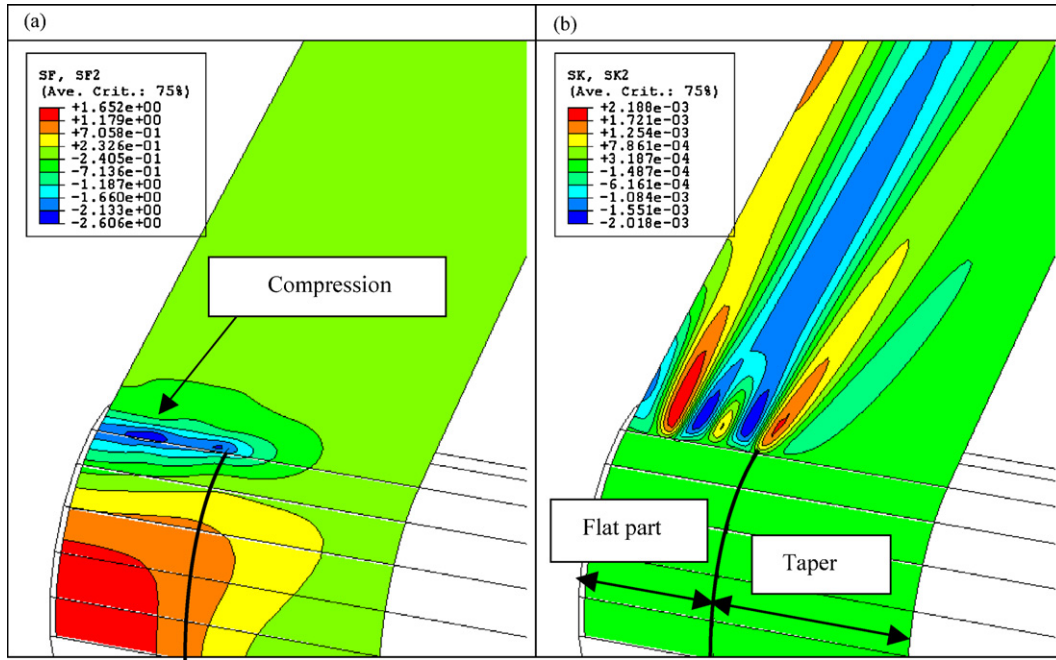


Fig. 7. Strip buckling before the strip motion. The sheet is handled by a tapered roll and subjected to a longitudinal tensile stress of 18 MPa (the corresponding membrane force is equal to 3.6 N/mm). (a) Transverse membrane force (N/mm) and (b) shell curvature ( $\text{mm}^{-1}$ ) are plotted for the following parameters: sheet thickness 0.2 mm, strip width 1000 mm, roll length 1900 mm, length of the flat part of the roll 400 mm, roll radius 220 mm, taper angle  $\rho = 1.33$  mm/m. An elastic behaviour is assumed for the strip: Young modulus  $E = 70,000$  MPa, Poisson ratio  $\nu = 0.3$ .

of magnitude. However, calculations have shown that compressive stresses stops increasing with the applied tensile load when the strip is in contact with the whole roll surface.

Due to the geometry of the strip, the critical buckling load is small (about 1 MPa). So, for tensile loads used in plants (about 10 MPa), the strip is in a far beyond buckling state. Nevertheless, because of the stabilizing effect of the global tension, the amplitude of buckles remains small. Typical post-buckling patterns are plotted in Fig. 7b. The shell curvature, which characterizes the stresses induced by the buckling, is maximum near the roll in the area where compressive stresses have significant values. Far from the roll, where compressive stresses have vanished, the buckles amplitude decreases slowly in the longitudinal direction

due to the stabilizing effects of the longitudinal tension and the sheet bending stiffness [3,5]. Thus, buckles develop even in an area where compressive stresses are negligible.

The transverse wavelength is much shorter than the longitudinal one. This typical feature of tensile buckling is due to a mechanism of wavelength selection induced by the longitudinal tensile stresses [4,5].

#### 4. From post-buckling to wrinkling

In this section, mechanisms leading to the accentuation of the post-buckling patterns during the strip motion are investigated.

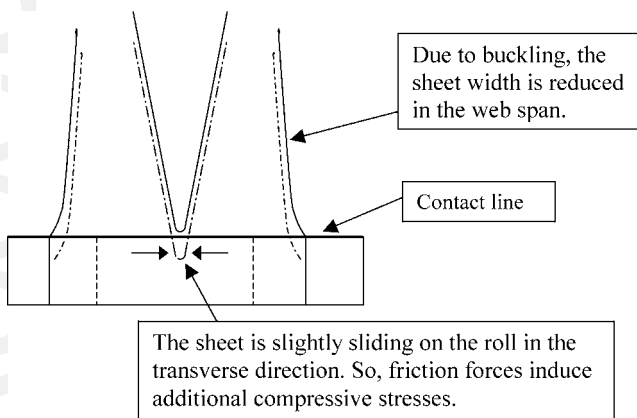


Fig. 8. Effect of friction during the strip displacement. Additional compressive stresses occur on the roll near the contact line. As a consequence, the post-buckling patterns become more pronounced.

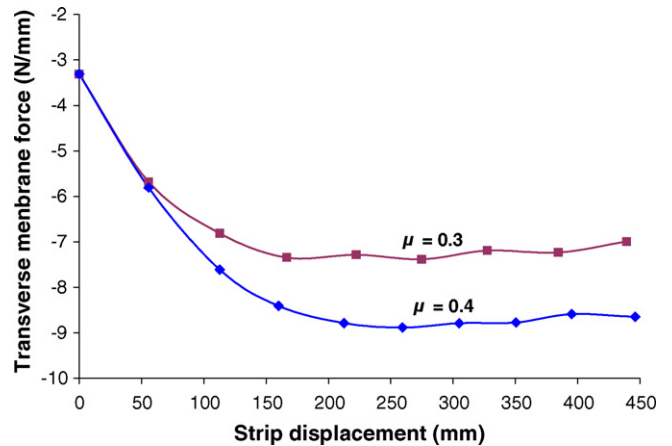


Fig. 9. Evolution of the magnitude of the transverse compressive membrane forces during the strip motion for two values of the friction coefficient ( $\mu = 0.3$  and 0.4). The applied tensile stress is equal to 25 MPa. Other data similar to those used for Fig. 7.

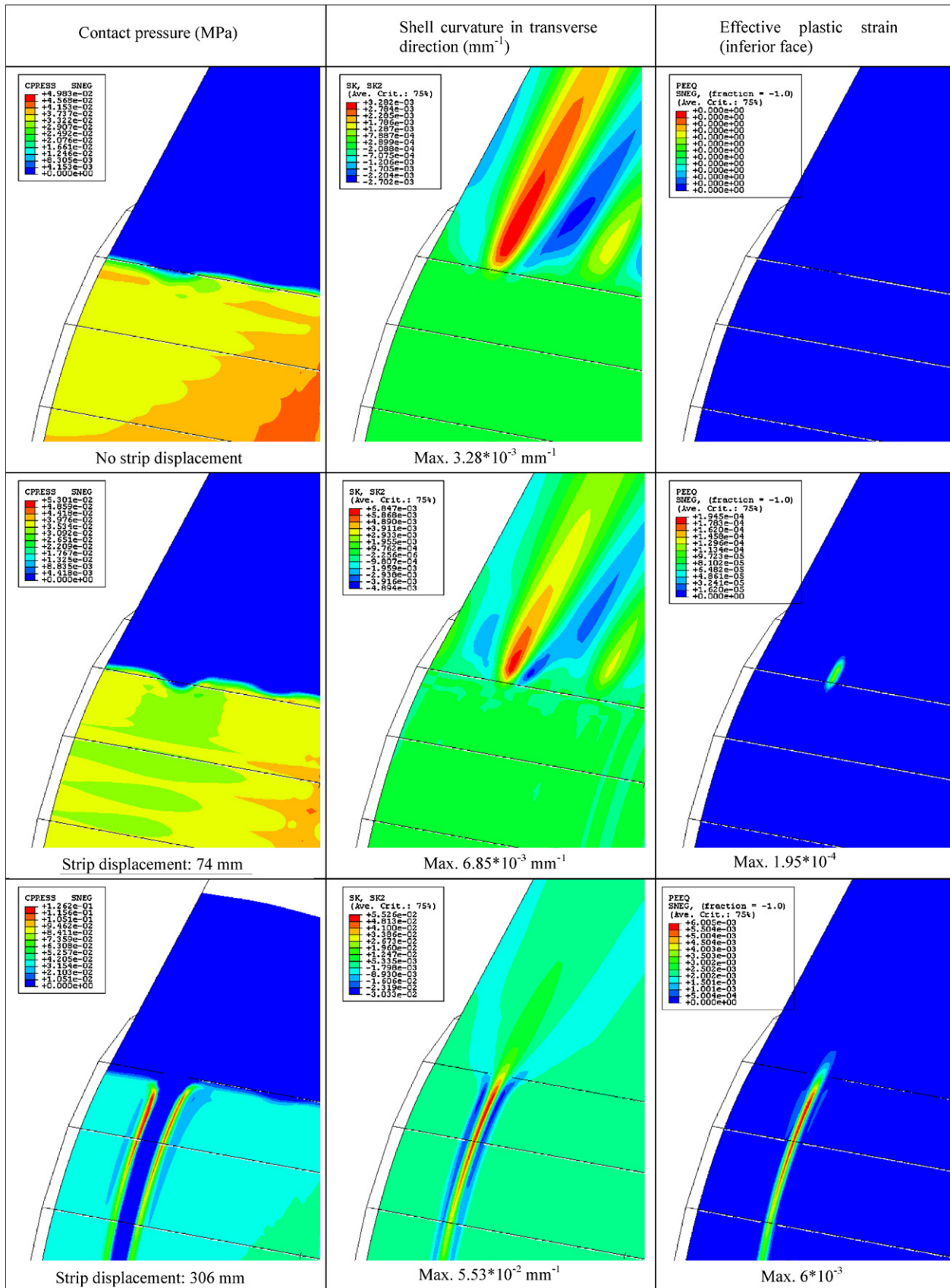


Fig. 10. Simulation of the formation of a wrinkle. These pictures show the sheet part coming into contact with the roll at three stages of the strip displacement. An elastic-plastic behaviour representative of some aluminium is considered: Young modulus  $E=70,000$  MPa, Poisson ratio  $\nu=0.3$ . The hardening curve is derived from tensile tests. Friction coefficient  $\mu=0.4$ . Applied stress  $\sigma_a=30$  MPa. The geometry as in Fig. 7 is adopted.

When the yield stress is not reached and contact between sheet and roll is frictionless, buckling patterns remain unchanged during the strip displacement. So, friction should be a key factor in the mechanism of wrinkling.

#### 4.1. Compressive stresses increase during the strip displacement

From numerical simulations, one observes that friction creates additional compressive stresses during the strip motion. The strip buckling induces small transverse displacements and thus reduces the strip width in the web span. When the sheet reaches the roll, it is slightly sliding on the roll in the transverse direction so as to retrieve its initial width (Fig. 8). As a consequence, friction forces act on the sheet and generate additional lateral compressive stresses during the strip displacement. These stresses depend on the friction coefficient and the tensile load, and have generally a larger magnitude than compressive stresses due to stretching. For the prescribed conditions of Fig. 9, compressive stresses increase by 110% during the strip displacement when the friction coefficient  $\mu$  is equal to 0.3 and by 160% for  $\mu = 0.4$ . Compressive stresses increase rapidly at the beginning of the strip motion and saturate when the displacement overcomes 200 mm. From other calculations not presented here, it was observed that, for thicker sheets, compression due to friction and strip motion becomes even more dominant. A consequence of the increase of compressive stresses during the strip displacement is the enhancement of the buckling patterns.

#### 4.2. A plastic cumulative mechanism causes the wrinkle formation

When the strip is elastic, the magnitude of the transverse shell curvature is almost proportional to the lateral compressive stress. Two situations can be encountered during the strip displacement. The case, where the material remains elastic or the plastic strain is limited, is first considered. Shell curvature and compressive stresses increases at the beginning of the motion but saturates for the same value of the prescribed displacement. In this case, wrinkles are not observed. Secondly, when larger plastic strains are generated during the strip motion, a plastic cumulative mechanism for the wrinkle formation occurs. The following description of this mechanism is proposed. Buckling induces a plastic strain gradient through the sheet thickness. As the strip reaches the roll, the difference in plastic strain through the thickness generates residual stresses, which amplify the buckling patterns in the web span. The amplitude of buckles increases leading to an enhanced plastic strain. Hence, the magnitude of the residual stresses increases. A catastrophic autocatalytic process is triggered. Due to this mechanism, shell curvature increases with the strip displacement even if compressive stresses have saturated. A wrinkle forms on the roll and propagates with the strip displacement.

Fig. 10 presents the different steps in the formation of a wrinkle. The first line corresponds to the post-buckling patterns before the strip displacement. As mentioned before, the strip buckling is due to the applied longitudinal tension and the roll

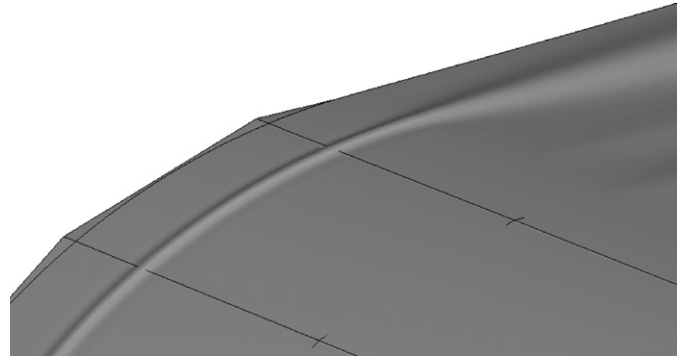


Fig. 11. Predicted wrinkle shape. Data are those of Fig. 10.

shape. During the early phase of the strip motion, an elastic accentuation of the buckling patterns is observed due to friction induced compressive stresses. After a prescribed displacement of 74 mm (Fig. 10, second line), the shell curvature has increased up to twice its initial value and the yield stress is reached. For a larger displacement, the plastic cumulative mechanism is triggered. A strong increase of the amplitude of the post-buckling patterns is observed. A wrinkle occurs during the strip motion. Once the wrinkle is fully developed (Fig. 10, third line), the level of shell curvature is 17 times greater than its initial value. The final shape of the wrinkle is plotted in Fig. 11. The wrinkle predicted by the finite element model is very similar to those observed in industrial processing lines. It takes place on the cylindrical part of the roll and its width is about 1 cm.

#### 4.3. Plastic cumulative mechanism and critical wrinkling load

The effect on the yield stress on the evolution of the shell curvature during the strip displacement is illustrated in Fig. 12. For low displacements, shell curvature does not depend on the yield stress since the strip remains elastic. The increase of shell curvature results from the increase of compressive stresses due to friction. When the displacement is over 150 mm, shell curvature

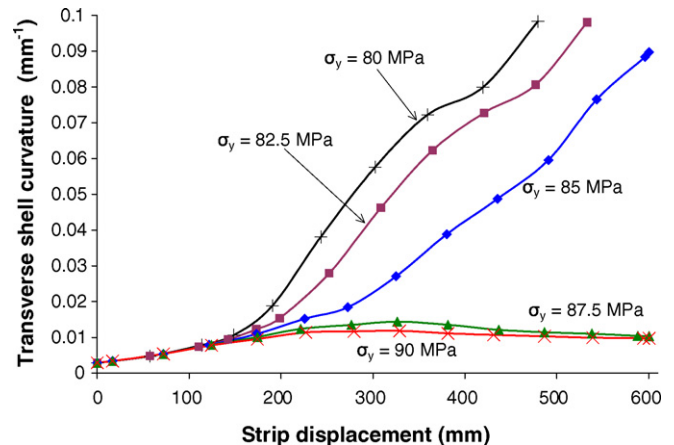


Fig. 12. Effect of the yield stress  $\sigma_y$  on the evolution of the transverse shell curvature (max value) during the strip displacement. The material is elastic-perfectly plastic. Applied tensile stress  $\sigma_a = 25$  MPa. Other data are as in Fig. 10.

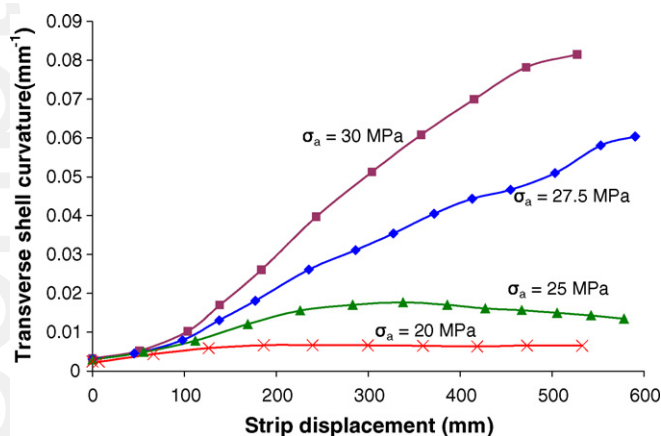


Fig. 13. Effect of the applied tensile stress  $\sigma_a$  on the evolution of the transverse shell curvature (max value) during the strip displacement. The configuration is identical to the one adopted for Fig. 10.

evolves differently depending on the yield stress of the material. For the largest values of the yield stress used in the calculations (87.5 and 90 MPa), the level of shell curvature remains moderate. Wrinkling does not occur. With the lowest yield stress (80, 82.5 and 85 MPa), shell curvature increases strongly when the yield stress is exceeded. The buckles amplification due to friction generates a level of plastic strain that triggers the plastic cumulative mechanism. Because of this mechanism, a small variation of the yield stress from 87.5 to 85 MPa induces a large increase of the shell curvature and the formation of a wrinkle. Therefore, from the proposed calculations, the plastic cumulative mechanism is not activated when the yield stress is over some limit, or equivalently when the plastic strain is under a critical value. Note that the critical level of plastic strain depends on the configuration, but is generally small (about 0.1%).

Next, the evolution of the shell curvature during the strip displacement for several traction levels is portrayed in Fig. 13. For low values of the applied tensile stress (20 and 25 MPa), the increase of shell curvature is moderate and almost proportional to the increase of compressive stresses. When the applied traction goes beyond a critical level, shell curvature increases strongly during the strip displacement. Hence, according to the simulations, the critical wrinkling load corresponds to the load level triggering the plastic cumulative mechanism. For the prescribed conditions of Fig. 13, the critical wrinkling load is between 25 and 27.5 MPa.

## 5. Conclusions

Numerical simulations have been performed in order to understand the formation of wrinkles during strip conveying in continuous processing lines. When a sheet is subjected to a longitudinal tension, the roll crown profile induces transverse compressive stresses and the sheet buckling. However, the tensile stresses induce a stabilizing effect and the amplitude of buckles remains small. The increase of compression during the strip motion is a key phenomenon in the wrinkle formation. This phenomenon is induced by friction forces acting on the sheet and leads to more pronounced post-buckling

patterns. As a consequence, the yield stress may be locally exceeded when the strip passes over a roll. In some cases, buckles evolve to create a wrinkle by a plastic cumulative mechanism. Note that these conclusions are based on the numerical results presented in this work. The simulations have been carried out on configurations which are representative of industrial processes. Nevertheless, it is likely that the mechanisms leading to the occurrence of wrinkles may be somewhat different for other configurations, e.g. with different materials or roll profiles.

The developed numerical model provides an estimation of critical wrinkling loads and can be used for the design of continuous processing lines in order to ensure wrinkle free operation. Currently, experiments are carried out in order to validate the numerical results.

Processing line designers try to prevent wrinkling by selecting suitable roll profiles. Nevertheless, the reduction of diameters variations is not always possible. For instance, in annealing lines, it is very difficult to prevent the thermal deformation of the rolls. Simulations have shown that friction has an important effect on wrinkling. So, another way to prevent wrinkling would be to select appropriate rolls materials and/or surface roughness in order to reduce friction coefficients.

In this study, buckling is due to the roll geometry. However, for some processes, buckling can also originate from other parameters like residual or thermal stresses. These additional factors can also be taken into account in finite element analyses [14].

## Acknowledgments

Some of the calculations were carried out on the SGI ORIGIN 3800 computer at the “Centre Informatique National de l’Enseignement Supérieur” (CINES). Technical support of CINES is gratefully acknowledged. The authors also thank Dr. S. Mercier for very helpful discussions.

## References

- [1] R.H. Segedin, I.F. Collins, C.M. Segedin, The elastic wrinkling of rectangular sheets, *Int. J. Mech. Sci.* 30 (1988) 719–732.
- [2] A.W. Liessa, E.F. Ayoub, Tension buckling of rectangular sheets due to concentrated forces, *J. Eng. Mech.* 115 (1989) 2749–2762.
- [3] N. Friedl, F.G. Rammerstorfer, F.D. Fisher, Buckling of stretched strips, *Comput. Struct.* 78 (2000) 185–190.
- [4] E. Cerda, L. Mahadevan, Geometry physics of wrinkling, *Phys. Rev. Lett.* 90 (2003) 074302.
- [5] N. Jacques, M. Potier-Ferry, On mode localisation in tensile plate buckling, *C.R. Mecanique* 333 (2005) 804–809.
- [6] T. Sasaki, T. Hira, H. Abe, F. Yangishima, Y. Shimoyama, K. Tahara, Control of strip buckling and snaking in continuous annealing furnace, *Kawasaki Steel Tech. Rep.* 9 (1984) 36–46.
- [7] T. Matoba, Effect of roll crown on heat buckling and strip walk in continuous annealing lines, *CAMP ISIJ* 5 (1992) 1459–1462.
- [8] H. Luo, W.S. Dunbar, J.E. Moore, Buckling analysis of a heated steel strip in a continuous annealing furnace, *J. Manuf. Sci. Eng.* 121 (1999) 326–335.
- [9] F.D. Fischer, F.G. Rammerstorfer, N. Friedl, W. Wieser, Buckling phenomena related to rolling and levelling of sheet metal, *Int. J. Mech. Sci.* 42 (2000) 1887–1910.



- [10] M. Marchand, Modélisation de la planéité en sortie de laminage des produits plats, Ph.D. Thesis, Ecole National Supérieure des Mines de Paris, 1999.
- [11] V. Gueydan, Modélisation numérique du flambage de bandes en acier dans les recuits continus, Ph.D. Thesis, University of Metz, 1997.
- [12] ABAQUS Inc., ABAQUS Manuals, Version 6.4, ABAQUS Inc., 2003.
- [13] A. Elias, F. Onno, G.F. Noville, D. Steiner, Amélioration du guidage des bandes et étude mécanique des phénomènes de formation des plis au recuit continu, Rapport de la Commission Européenne EUR 18796, ISBN 92-828-5413-2, 1999.
- [14] N. Jacques, Modélisation et étude du plissement des tôles lors de leur transport en continu dans les usines sidérurgiques, Ph.D. Thesis, University of Metz, 2004.